Critical exponents of a three-dimensional O(4) spin model

K. Kanaya and S. Kaya
Institute of Physics, University of Tsukuba, Ibaraki 305, Japan
(Received 1 September 1994)

By Monte Carlo simulation we study the critical exponents governing the transition of the three-dimensional classical O(4) Heisenberg model, which is considered to be in the same universality class as finite-temperature QCD with two massless flavors. We use the single-cluster algorithm and the histogram reweighting technique to obtain observables at the critical temperature. After estimating an accurate value of the inverse critical temperature $K_c = 0.9360(1)$, we make nonperturbative estimates for various critical exponents by a finite-size scaling analysis. We find $\nu = 0.7479(90)$, $\beta/\nu = 0.5129(11)$, and $\gamma/\nu = 1.9746(38)$. They are in excellent agreement with those obtained by perturbation theory with errors reduced to about one-half.

PACS number(s): 11.15.Ha, 12.38.Gc, 75.10.Hk, 75.40.Mg

I. INTRODUCTION

The finite temperature chiral phase transition of QCD is very important in the study of phase transitions in the early Universe and in the investigation of heavy ion collisions at high energy. At present, this transition is studied mainly using the Monte Carlo method on the lattice. Pisarski and Wilczek [1,2] suggested that QCD with two massless flavors, which is considered to be an approximation of the real world, belongs to the same universality class as three-dimensional (3D) four-component Heisenberg models, if the finite temperature chiral transition of $N_f = 2$ QCD is second order. Then, the chiral transition of $N_f = 2$ QCD has the same critical exponents as the 3D O(4) Heisenberg model.

Simulations of lattice QCD for $N_f = 2$ suggest that the chiral transition is a second-order transition for staggered fermions [3] and for Wilson fermions [4]. The study towards a precise measurement of the critical exponents of $N_f = 2$ QCD has just begun [5]. In the verification that the O(4) Heisenberg model belongs to the same universality class, there is a problem that both Wilson fermions and staggered fermions on the lattice do not have the full chiral symmetry, which is expected to be restored only in the continuum limit. Conversely, however, we could consider that, assuming universality, chiral symmetry is restored on the lattice sufficiently when the exponents agree with those of the 3D O(4) Heisenberg model.

Therefore an accurate calculation of the critical exponents of the 3D O(4) Heisenberg model is quite important. For this model the best estimation of critical exponents has been made with perturbation theory up to seven loops combined with a Padé-Borel-Leroy resummation method [6].

In this work we simulate the 3D O(4) Heisenberg model by the Monte Carlo method and make a nonperturbative estimation of several critical exponents. We use the single-cluster Monte Carlo update algorithm which recently has been used for the simulation of spin systems: Wolff formulated this algorithm by modifying the multiple-cluster algorithm by Swendsen and Wang [7] and applied it to continuous spin models [8–10]. Recent applications of the multiple- and single-cluster algorithms to two- and three-dimensional spin models have demonstrated their advantage in the computation time to the usual local update algorithms. Among global algorithms, the single-cluster algorithm is shown to be superior to the multiple-cluster algorithm for three-dimensional spin models [11,12]. Therefore, we apply the single-cluster algorithm in this study.

In Sec. II the model and the method of simulation are described. In Sec. III we estimate the transition point from the crossing point of the Binder cumulant and compute the critical exponents at the transition point making use of the histogram reweighting technique. We also check the consistency of the results by independent measurements of the critical temperature and several exponents. We then compare our exponents with those of perturbation theory. Our conclusion is given in Sec. IV.

II. THE MODEL AND THE METHOD

The partition function Z and the energy E of the 3D O(4) Heisenberg model are defined by

$$Z = \prod_{\boldsymbol{x}} \int [d\vec{s}]\, e^{(-KE)},$$

$$E = \sum_{\boldsymbol{x},\hat{\imath}} \{1 - \vec{s}(\boldsymbol{x}) \cdot \vec{s}(\boldsymbol{x} + \hat{\imath})\}, \tag{1}$$

where K is the inverse temperature and $\vec{s}(\boldsymbol{x})$ is a four-dimensional unit spin at the lattice site $\boldsymbol{x}$. $\hat{\imath}$'s are the unit steps in three coordinate directions. We use three-dimensional simple cubic lattices with the volume $V = L^3$ with $L = 8$, 10, 12, 14, 16, 24, and 32, and employ periodic boundary conditions.

We choose two simulation points for each L except for $L = 10$: One is $K = 0.935$, which is a rough estimate for the transition point by our preparatory simulation. Another simulation point is chosen for each L at

0556-2821/95/51(5)/2404(7)/$06.00

TABLE I. Simulation parameters and statistics. $K_{\rm simu}$ is the simulation point; "iteration" is the number of cluster updates by single-cluster algorithm; $\langle C \rangle$ is the mean cluster volume; "sweep" is the number of updates in Metropolis-equivalent units, i.e., in units of updates of whole spins on the lattice: sweeps = iterations $\times \langle C \rangle / V$, where $V = L^3$ is the lattice volume; τ_χ is the autocorrelation time in sweeps for the magnetic susceptibility χ defined by (18); $N_{\rm indep}$ is the number of independent data: $N_{\rm indep}$ =sweeps/τ_χ; and χ is the magnetic susceptibility measured at $K_{\rm simu}$.

L	$K_{\rm simu}$	Iterations/10^3	$\langle C \rangle$	Sweeps/10^3	τ_χ	$N_{\rm indep}/10^3$	χ
8	0.892	3000	31.6	185	1.95	95	
8	0.935	3000	51.1	299	2.49	120	65.48(8)
10	0.935	4400	78.7	346	2.55	136	101.82(12)
12	0.910	4000	67.3	156	1.98	80	
12	0.935	6000	113.2	393	2.48	159	145.24(16)
14	0.912	1400	88.0	45	1.82	25	
14	0.935	6000	154.5	338	2.47	136	196.08(23)
16	0.920	3000	129.5	95	1.98	23	
16	0.935	5200	197.4	251	2.32	108	254.92(33)
24	0.926	1500	280.9	30	1.87	16	
24	0.935	2400	427.1	74	2.21	34	554.4(13)
32	0.928	1500	449.5	21	1.62	13	
32	0.935	5600	719.1	123	1.95	63	958.1(17)

the maximum point of the susceptibility estimated by a preparatory simulation. Our simulation parameters are compiled in Table I. We use the data at $K = 0.935$ for the calculation of the transition point as well as the analyses of finite-size scaling with the histogram reweighting technique and use the data at the maximum of the susceptibility for a check of the consistency of our results.

The magnetization and the energy are measured every 10 cluster updates by the single-cluster algorithm and stored on the disk. Several million cluster updates are performed for each simulation point. From the autocorrelation time we measured (see the following section) this corresponds to about one hundred thousand independent data for each point, as compiled in Table I. We estimate errors by the jackknife procedure. We study the bin-size dependence of errors and choose a sufficiently large bin size such that errors become stable. The resulting bin sizes are consistent with the values of autocorrelation time estimated independently. All the jobs take 23 hours with HITAC S820/80.

We use the histogram reweighting method [13] to calculate the observables in a region of K around the simulated point $K_{\rm simu}$. The region of K in which the histogram reweighting method is applicable can be determined by the magnitude of the shift of energy value: If the peak position of a reweighted energy distribution, $E_{\rm peak}(K)$, locates away from the peak position of the original distribution, $E_{\rm peak}(K_{\rm simu})$, then the statistical errors for averages computed with the reweighted distribution become large correspondingly. Limited statistics near the tails of measured histograms also lead to the danger of a large underestimation of the errors there. We study the effect of reweighting and observe that, with our statistics, many errors for the observables we study become rapidly large and the histogram becomes rapidly notched when K gets outside the region where the height of the original energy histogram at $E_{\rm peak}(K)$ is larger than one-third of the peak height. Although several computed errors, such as the error for the Binder cumulant discussed below, sometimes remain small even outside this range, we find that the result is not consistent with the result of a direct simulation there. We therefore limit ourselves to apply the histogram reweighting method only up to the point where the height of the original energy histogram at $E_{\rm peak}(K)$ decreases to one-third of the peak height. A similar criterion is used also in Ref. [14].

A. Algorithm

We use the single-cluster algorithm formulated by Wolff [8]. This is a global update algorithm whose advantage is that the autocorrelation time and the dynamical exponent are both much smaller than those of the local update algorithm as discussed below.

The autocorrelation function $A_{\mathcal{O}}(k)$ for an observable $\mathcal{O}$ is defined by

$$A_{\mathcal{O}}(k) = \frac{\rho_{\mathcal{O}}(k)}{\rho_{\mathcal{O}}(0)} ,$$
$$\rho_{\mathcal{O}}(k) = \langle \mathcal{O}_i \mathcal{O}_{i+k} \rangle - \langle \mathcal{O}_i \rangle^2 , \quad (2)$$

with $\mathcal{O}_i$ being the ith measurement of $\mathcal{O}$. The autocorrelation time $\tau_{\mathcal{O}}$ given by integrating the autocorrelation function

$$\tau_{\mathcal{O}} = \sum_{k=1}^{\infty} A_{\mathcal{O}}(k) \quad (3)$$

diverges in the critical region as $\tau_{\mathcal{O}} \propto \xi^z$, where ξ is the correlation length. The exponent z is called as dynamical exponent. On finite lattices in the critical region, ξ is replaced by the lattice length L:

$$\tau_{\mathcal{O}} \propto L^z . \quad (4)$$

This lattice size dependence of $\tau_{\mathcal{O}}$ is the origin of the "critical slowing down" which makes it difficult to get high effective statistics in the critical region on large lattices. We should use an algorithm with a small dynamical exponent. It is known that the local update algorithms, such as the Metropolis algorithm, have $z \sim 2$ independent of the model and the details of the update algorithm. For example, $z = 1.94(6)$ is obtained for the 3D O(3) Heisenberg model with a Metropolis algorithm [15]. Use of a global update algorithm is required to get a smaller z. It is reported in Refs. [11,14,16] that z with single-cluster algorithm for the 3D Ising model is about 0.2 and that for the 3D O(3) Heisenberg model is about 0. As presented in the next section, our result of z for the 3D O(4) Heisenberg model is also consistent with 0.

The single-cluster update for the $O(n)$ Heisenberg model is described in Refs. [8,17]. In order to test the efficiency of the algorithm and to test our program code for the single-cluster update, we simulate the 3D Ising and the 3D O(3) Heisenberg model. Our results are completely consistent with Refs. [11,14], including the results for susceptibility, dynamical exponent, and critical exponents.

III. RESULTS

A. Autocorrelation time and energy distribution

Our results for the autocorrelation time τ_χ for the magnetic susceptibility χ, defined by (18), are compiled in Table I. We find that τ_χ in Metropolis-equivalent units, i.e., in units of updates for V spins, stays almost constant or rather decreases with the increase of the lattice size. This implies that the dynamical exponent is 0 or slightly smaller than 0. A similar result is obtained also for the O(3) Heisenberg model [14].

The measured energy distribution shown in Fig. 1 is a

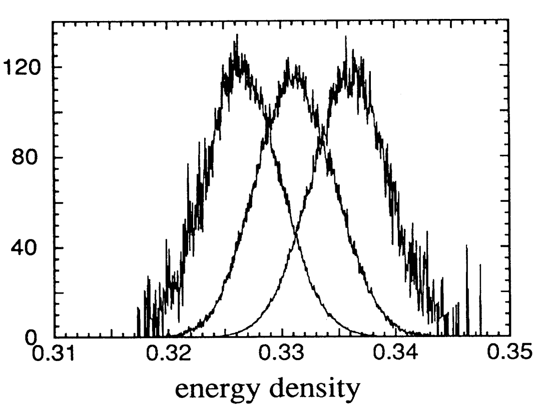

FIG. 1. Histogram of energy density for $L = 32$ near the critical coupling. Each distribution is normalized to unit area. Histograms are for $K = 0.929$, 0.935, and 0.939 from the left to the right, respectively. The histograms for $K = 0.929$ and 0.939 are obtained by reweighting the measured histogram at $K = 0.935$.

Gaussian-type with a single peak. The continuous shift of the distribution with temperature over the expected critical region is consistent with a second-order phase transition in accordance with the results of perturbation theory. Final confirmation of the order of the transition is done with the values of the critical exponents discussed below.

In 2D spin models [8,10] and also in the 3D O(3) Heisenberg model [14], the mean cluster volume $\langle C \rangle$ is found to be proportional to the magnetic susceptibility χ in the scaling region independent of the lattice size. This suggests that the spin correlation length is approximately explained by the size distribution of clusters. From the values listed in Table I, we find a similar property: $\langle C \rangle K/\chi \approx 0.72$–$0.73$.

B. Critical temperature

An accurate calculation of critical exponents requires a precise determination of the inverse critical temperature K_c. An efficient method to determine K_c for a second-order transition is to measure the Binder cumulant [18] for various system sizes and to locate the cross point in the space of K. On sufficiently large lattices where subleading corrections from the finite lattice size L are ignored, the Binder cumulant $U_L(K)$ defined by

$$U_L(K) = 1 - \frac{1}{3}\frac{\langle m^4\rangle}{\langle m^2\rangle^2}, \qquad \vec{m} = \frac{1}{V}\sum_{\boldsymbol{x}} \vec{s}(\boldsymbol{x}) \,, \tag{5}$$

becomes independent of L at the transition point K_c [18]:

$$\frac{U_{L'}(K_c)}{U_L(K_c)} = 1, \tag{6}$$

and the slope of $U_L(K)$ in K at K_c increases as L becomes large. In Fig. 2 are shown our results of the Binder cumulant near the crossing point. The values for $U_L(K)$ are obtained with the histogram method using the data at $K = 0.935$.

The deviation from the relation (6) observed in Fig. 2 can be explained by the finite-size confluent corrections. The leading L'/L dependence in the deviation of the crossing point K^* from the critical point K_c is estimated by Binder [18] as

$$\frac{1}{K_c} - \frac{1}{K^*} \propto \frac{1}{\ln b}, \tag{7}$$

where $b = L'/L$.

We plot $(1/\ln b, 1/K^*)$ for $L = 8$, 10, 12, and 14 in Fig. 3. The errors for $1/K^*$ are computed from the jackknife errors for $U_L(K)$. The solid lines in Fig. 3 represent the results of a linear least-squares fit for each L. We find that the correction with $1/\ln b$ is smaller than that of the 3D O(3) Heisenberg model [14]. The extrapolation of $1/K^*$ to the point $1/\ln b = 0$ for each L gives the values for $1/K_c(L)$: $1/K_c(8) = 1.06841(21)$,

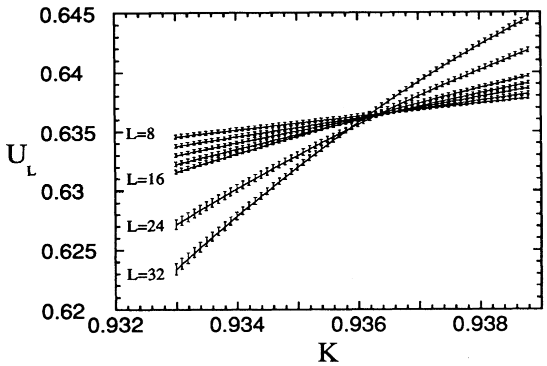

FIG. 2. The Binder cumulant U_L as a function of the inverse temperature K for L = 8, 10, 12, 14, 16, 24, and 32. $U_L(K)$ is computed with the histogram reweighting method using the data at $K = 0.935$.

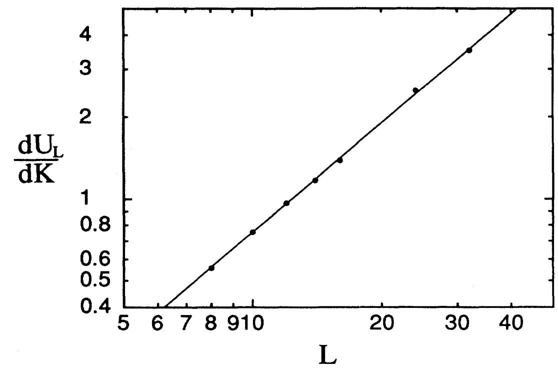

FIG. 4. Scaling of the slope dU_L/dK of the Binder cumulant at $K_c = 0.9360(1)$ as a function of the lattice size L. The slope of the solid line given by a linear least-square fit leads to an estimate of the critical exponent $1/\nu = 1.337(16)$. The jackknife errors for dU_L/dK are smaller than the size of symbols.

$1/K_c(10) = 1.06832(26)$, $1/K_c(12) = 1.06833(26)$, and $1/K_c(14) = 1.06826(34)$. All of them are consistent with each other. The mean value of these results is $1/K_c = 1.06835(13)$. A similar fit for all L with a common parameter $1/K_c$ gives the value $1/K_c = 1.06836(14)$, which completely agrees with the mean value. We quote hereafter

$$\frac{1}{K_c} = 1.06835(13), \tag{8}$$

$$K_c = 0.9360(1). \tag{9}$$

C. The critical exponent ν

The slope for $\left.\frac{dU_L}{dK}\right|_{K=K_c}$ is known to scale with a critical exponent ν as [18]

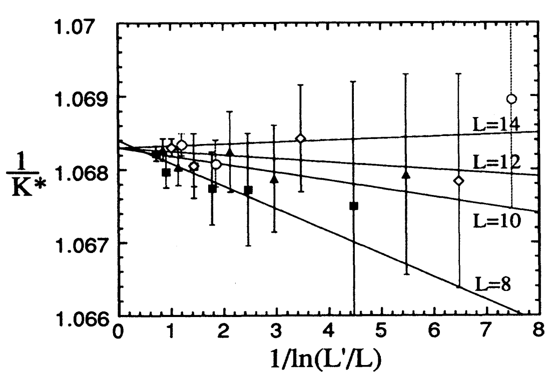

FIG. 3. The crossing point of Binder cumulants $U_L(K)$ and $U_{L'}(K)$ for L = 8 (squares), 10 (triangles), 12 (diamonds), and 14 (circles) with different L'. Solid lines correspond to linear least-squares fits for each L. The critical coupling is estimated as $K_c = 0.9360(1)$ by extrapolating these lines to the limit $1/\ln(L'/L) = 0$.

$$\left.\frac{dU_L}{dK}\right|_{K=K_c} \sim L^{1/\nu}\,. \tag{10}$$

Using the relation

$$\frac{dU_L}{dK} = (1 - U_L)\left\{\langle E\rangle - 2\frac{\langle m^2 E\rangle}{\langle m^2\rangle} + \frac{\langle m^4 E\rangle}{\langle m^4\rangle}\right\}, \tag{11}$$

we calculate $dU_L/dK|_{K=K_c}$ at the estimated $K_c = 0.9360$. In Fig. 4, we plot dU_L/dK as a function of L. From the slope of the solid line in this logarithmic plot we find

$$\frac{1}{\nu} = 1.337(16), \tag{12}$$

$$\nu = 0.7479(90), \tag{13}$$

by a least-squares fit. We repeat the analysis by varying K_c within our estimated error, 0.9360(1), and find that the results for ν are completely consistent with the result given here.

The scaling relation (10) requires a sufficiently large L to ignore the subleading corrections. In order to test if our values of L are large enough, we repeat the fits excluding the data for the smallest size $L = 8$, and for $L = 8$ and $L = 10$. We obtain $1/\nu(L = 8 \text{ excluded}) = 1.344(36)$ and $1/\nu(L = 8 \text{ and } 10 \text{ excluded}) = 1.333(51)$, respectively. Because these results are completely consistent with $1/\nu$ with all data, we conclude that $L = 8$ is sufficiently large to extract scaling properties.

D. The result for β/ν

The scaling relation of the magnetization $\langle|m|\rangle$ at K_c is given by

$$\langle|m|\rangle_{K_c} \sim L^{-\beta/\nu}\,. \tag{14}$$

We study the scaling of $\langle|m|\rangle_{K_c}$ at $K_c = 0.9360$ and obtain $\beta/\nu = 0.5129(7)$ from the slope of the fitted line in

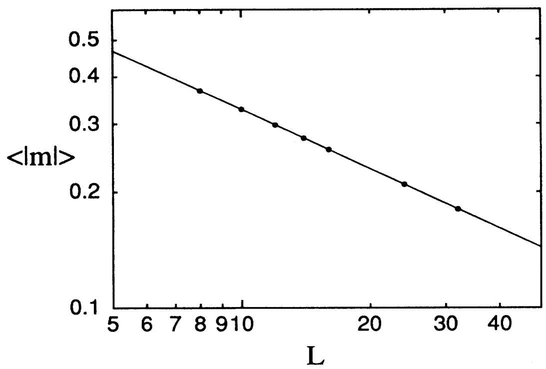

FIG. 5. Magnetization $\langle |m| \rangle$ at $K_c = 0.9360(1)$ as a function of the lattice size L. A least-squares fit gives $\beta/\nu = 0.5129(7)$. The jackknife errors for $\langle |m| \rangle$ are smaller than 1/10 of the size of symbols.

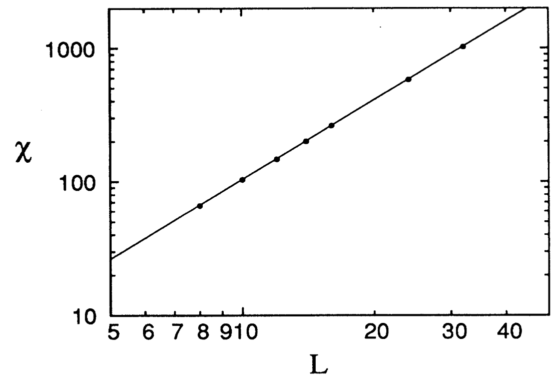

FIG. 6. Susceptibility χ at $K_c = 0.9360(1)$ as a function of L. A least-squares fit gives $\gamma/\nu = 1.9746(15)$. The jackknife errors for $\chi(K_c)$ are smaller than 1/10 of the size of symbols.

Fig. 5. The fits excluding $L = 8$, and $L = 8$ and 10 give the results consistent with this value [$\beta/\nu(L = 8$ excluded) $= 0.5130(15)$ and $\beta/\nu(L = 8$ and 10 excluded) $= 0.5127(21)$]. Unlike the case of ν in the previous subsection, we find that the effect of the error of K_c on the estimate of β/ν is larger than the statistical error 0.0007 at $K_c = 0.9360$:

$$\frac{\beta}{\nu}(K_c = 0.9359) - \frac{\beta}{\nu}(K_c = 0.9360) = 0.0009\ ,$$
$$\frac{\beta}{\nu}(K_c = 0.9360) - \frac{\beta}{\nu}(K_c = 0.9361) = 0.0011\ . \tag{15}$$

Therefore we should use the value 0.0011 for the error of β/ν:

$$\frac{\beta}{\nu} = 0.5129(11)\ . \tag{16}$$

Combined with our estimate for ν, we have

$$\beta = 0.3836(46)\ . \tag{17}$$

E. The result for γ/ν

For $K \leq K_c$ the susceptibility χ is defined by

$$\chi = VK\left\langle m^2 \right\rangle . \tag{18}$$

The scaling relation of χ at K_c is given by

$$\langle \chi \rangle_{K_c} \sim L^{\gamma/\nu}\ . \tag{19}$$

With a similar method as in the previous sections, we obtain for $K_c = 0.9360$, $\gamma/\nu = 1.9746(15)$ from the slope of the fitted line in Fig. 6. Again, the value of γ/ν depends strongly on the choice of K_c:

$$\frac{\gamma}{\nu}(K_c = 0.9360) - \frac{\gamma}{\nu}(K_c = 0.9359)$$
$$\cong \frac{\gamma}{\nu}(K_c = 0.9361) - \frac{\gamma}{\nu}(K_c = 0.9360) \tag{20}$$
$$= 0.0038\ . \tag{21}$$

Therefore we quote

$$\frac{\gamma}{\nu} = 1.9746(38)\ . \tag{22}$$

Combined with our estimate of ν, we get

$$\gamma = 1.477(18)\ . \tag{23}$$

Using our independent results for β/ν and γ/ν, we can check the hyperscaling relation

$$\frac{\beta}{\nu} + \frac{1}{2}\frac{\gamma}{\nu} - \frac{d}{2} = 0\ . \tag{24}$$

We find

$$\text{LHS} = 0.0002 \pm 0.003 \tag{25}$$

that is consistent with zero to $\sim 10^{-3}$.

F. Scaling of χ^c and $K_{\chi^c_{\max}}$

To make a further check of our results for exponents, we study the finite-size scaling property of the peak of the connected susceptibility χ^c:

$$\chi^c = VK(\langle m^2 \rangle - \langle |m| \rangle^2), \tag{26}$$

whose maximum value is expected to behave as

$$\chi^c_{\max} \sim L^{(\gamma/\nu)_c}. \tag{27}$$

Here we add a suffix c for the exponent to make clear the way it is defined. Because the pseudocritical coupling constant $K_{\chi^c_{\max}}$ where χ^c gets its maximum value is found to be slightly off the range of the applicability of the histogram reweighting method for the data at K_c (see the discussion in Sec. II), we carry out new simulations at $K \simeq K_{\chi^c_{\max}}$ listed in Table I determined by a preparatory simulation. With the histogram method applied to these new data we estimate accurate values for $\chi^c_{\max}$ and $K_{\chi^c_{\max}}$ (see Table III). From a least-squares fit shown in Fig. 7, we obtain

$$(\gamma/\nu)_c = 1.996(8)\ . \tag{28}$$

TABLE II. Critical exponents of the three-dimensional O(4) Heisenberg model obtained by perturbation theory [6,2] and by this study. In perturbation theory, independent calculations are done for ν and η. In this study, γ/ν, β/ν, and ν are determined independently. Other exponents are calculated using (hyper)scaling relations.

	Perturbation theory	This study
$\gamma/\nu = 2 - \eta$	1.97(1)	1.9746(38)
β/ν	0.515(5)	0.5129(11)
ν	0.73(2)	0.7479(90)
γ	1.44(4)	1.477(18)
β	0.38(1)	0.3836(46)
δ	4.82(5)	4.851(22)
$\alpha = 2 - d\nu$	−0.19(6)	−0.244(27)

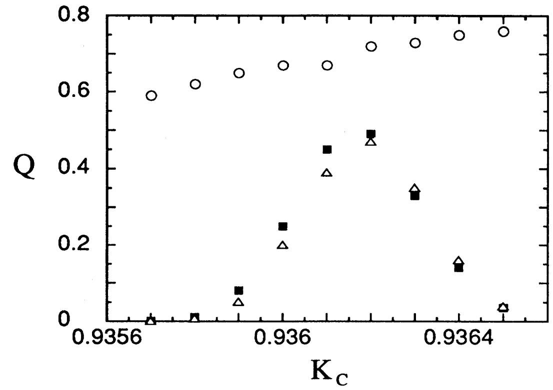

FIG. 8. Q values of least-squares fits for dU_L/dK (circles), $\langle|m|\rangle$ (squares), and χ (triangles) for various fixed K_c.

This value is slightly larger than that from the scaling of χ, 1.9746(38), given in (22). The same tendency is observed for the O(3) Heisenberg model [14,19]. Because the quality of the fit for χ is better than that for $\chi^c_{\max}$, we quote (22) for the value of γ/ν.

The scaling property of the pseudocritical coupling $K_{\chi^c_{\max}}$ provides us another test of our results:

$$K^{-1}_{\chi^c_{\max}} \sim K_c{}^{-1} + aL^{-1/\nu} . \tag{29}$$

Using our estimate $1/\nu = 1.337$, we fit the data with two parameters $K_c{}^{-1}$ and a to obtain

$$K_c = 0.9360(2). \tag{30}$$

This value is consistent with our K_c from the crossing points of the Binder cumulant.

G. Restriction of the transition point by Q value

The scaling relations (10), (14), and (19) require that the estimated value of K_c is close enough to the real transition point. If we fix K_c far from the real transition point in these scaling relations the data will no longer fit them well.

The quality of a least-squares fit is determined by the Q value [20]:

$$Q(\chi^2, n) = \int_{\chi^2}^{\infty} dt \left(\frac{t}{2}\right)^{\frac{n}{2}-1} e^{-t/2}, \tag{31}$$

where χ^2 is the weighted sum of squared deviations of data from the fit, and n = (number of data points) − (number of fit parameters) is the degree of freedom for the fit. We may consider that the fitting procedure is appropriate if $0.1 \le Q \le 0.9$. If, on the other hand, $Q < 0.1$ something is wrong: the error of data may be underestimated or the fitting function may be incorrect, and if $Q > 0.9$ error of data may be overestimated or we have too many fit parameters.

In the present case, if we fix K_c far from the real transition point, the quality of the scaling fits must become low so that the Q value decreases to a value less than 0.1. In Fig. 8 the Q values of our finite-size scaling fits for dU_L/dK, $\langle|m|\rangle$ and χ are plotted as a function of K_c. We find that Q value for dU_L/dK is not so sensitive on K_c, while the Q values for $\langle|m|\rangle$ and χ depend sensitively on K_c. This difference of the dependence on K_c between

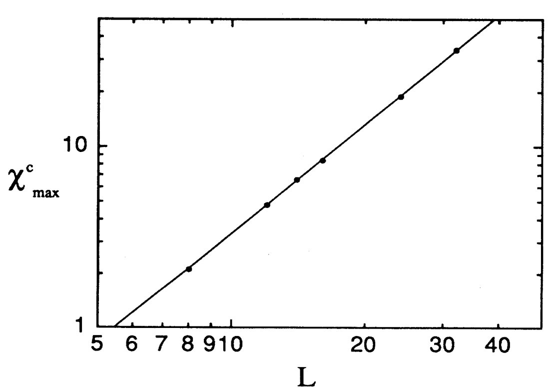

FIG. 7. The maximum height of the connected susceptibility $\chi^c_{\max}$. A least-squares fit gives $(\gamma/\nu)_c = 1.996(8)$. The jackknife errors for $\chi^c_{\max}$ are smaller than 1/5 of the size of symbols.

TABLE III. Results for the pseudocritical coupling $K_{\chi^c_{\max}}$ and the maximum values $\chi^c_{\max}$ of the connected susceptibility χ^c. The K dependence of χ^c is determined by the histogram reweighting method using the data simulated at K_{simu} on an L^3 lattice.

L	K_{simu}	$K_{\chi^c_{\max}}$	$\chi^c_{\max}$
8	0.892	0.8907(37)	2.118(09)
12	0.910	0.9109(05)	4.793(28)
14	0.912	0.9144(06)	6.577(48)
16	0.920	0.9183(08)	8.390(46)
24	0.926	0.9253(06)	18.89(16)
32	0.928	0.9289(01)	33.97(32)

dU_L/dK and $\langle|m|\rangle$, χ is the same as that observed for the O(3) Heisenberg model [14]. From the condition that $Q \leq 0.1$ we have

$$0.9359 \leq K_c \leq 0.9364. \tag{32}$$

This provides us another consistency check of our analyses. The value obtained from the crossing point of the Binder cumulant $K_c = 0.9360(1)$ is well included in this region.

H. Comparison with perturbation theory

The critical exponents obtained in this work are compiled in Table II together with the values by perturbation theory [6,2]. In our results, the exponents γ/ν, β/ν, and ν are determined independently, and α and δ are calculated using (hyper)scaling relations with the value of other exponents. In the results of perturbation theory, η and ν are estimated independently and other exponents are calculated with η and ν. Our results are completely consistent with those of perturbation theory with the errors reduced to about one-half.

IV. CONCLUSION

We simulated the three-dimensional O(4) Heisenberg model by applying the single-cluster algorithm, which reduces the dynamical exponent to about zero. The histogram reweighting method with high statistics data confirmed that the transition is second order for this model. We performed a precise estimation of the critical point to get $K_c = 0.9360(1)$ from the crossing point of the Binder cumulant. The critical exponents were calculated using finite-size scaling at K_c. The exponents obtained, which are summarized in Table II, are completely consistent with those of perturbation theory with the errors reduced to about one-half.

ACKNOWLEDGMENTS

We are grateful to Y. Iwasaki and A. Ukawa for valuable discussions and helpful suggestions. Numerical calculations were done on HITAC S820/80 at the National Laboratory for High Energy Physics (KEK). We would like to thank members of KEK for their hospitality and strong support, and members of the Theory Group of the Institute of Physics, University of Tsukuba, for innumerable discussions and encouragements. This project was in part supported by a Grant-in-Aid of the Ministry of Education, Science and Culture (No.6206001 and 02402003).

[1] R. Pisarski and F. Wilczek, Phys. Rev. D **29**, 338 (1984).
[2] F. Wilczek, Int. J. Mod. Phys. A **7**, 3911 (1992); K. Rajagopal and F. Wilczek, Nucl. Phys. **B399**, 395 (1993).
[3] M. Fukugita, H. Mino, M. Okawa, and A. Ukawa, Phys. Rev. D **42**, 2936 (1990); A. Vaccarino, in *Lattice'90*, Proceedings of the International Symposium, Tallahassee, Florida, edited by U. M. Heeler, A. D. Kennedy, and S. Sanielevici [Nucl. Phys. B (Proc. Suppl.) **20**, 263 (1991)].
[4] Y. Iwasaki, K. Kanaya, S. Sakai, and Y. Yoshié, in *Lattice'92*, Proceedings of the International Symposium, Amsterdam, the Netherlands, edited by J. Smit and P. van Baal [Nucl. Phys. B (Proc. Suppl.) **30**, 327 (1993)].
[5] F. Karsch, Phys. Rev. D **49**, 3791 (1994); F. Karsch and E. Laermann, *ibid.* **50**, 6954 (1994).
[6] G. Baker, D. Meiron, and B. Nickel, Phys. Rev. B **17**, 1365 (1978); *Compilation of 2-pt. and 4-pt. graphs for continuous spin models*, University of Guelph Report, 1977 (unpublished).
[7] R. H. Swendsen and J.-S. Wang, Phys. Rev. Lett. **58**, 86 (1987); J.-S. Wang and R. H. Swendsen, Physica A **167**, 565 (1990).
[8] U. Wolff, Phys. Rev. Lett. **62**, 361 (1989).
[9] U. Wolff, Phys. Lett. B **222**, 473 (1989); **248**, 335 (1990).
[10] U. Wolff, Nucl. Phys. **B322**, 759 (1989); **B334**, 581 (1990).
[11] U. Wolff, Phys. Lett. B **228**, 379 (1989).
[12] P. Tamayo, R. C. Brower, and W. Klein, J. Stat. Phys. **58**, 1083 (1990); M. Hausenbusch and S. Meyer, Phys. Lett. B **241**, 238 (1990); W. Janke, Phys. Lett. A **148**, 306 (1990).
[13] I. R. McDonald and K. Singer, Discuss. Faraday Soc. **43**, 40 (1967); A. M. Ferrenberg and R. H. Swendsen, Phys. Rev. Lett. **61**, 2635 (1988); **63**, 1195 (1989).
[14] C. Holm and W. Janke, Report Nos. FUB-HEP 19/92, and HLRZ 77/92 (September 1992)(most detailed); Report Nos. FUB-HEP 9/92, and HLRZ 56/92, Berlin/Jülich (August 1992); in *Lattice '92* [4], p. 846.
[15] P. Peczak and D. P. Landau, J. Appl. Phys. **67**, 5427 (1990).
[16] J.-S. Wang, Physica A **164**, 240 (1990).
[17] H. G. Evertz, in *Lattice '91*, Proceedings of the International Symposium, Tsukuba, Japan, edited by M. Fukugita *et al.*[Nucl. Phys. B (Proc. Suppl.) **26**, 620 (1992)].
[18] K. Binder, Z. Phys. B **43**, 119 (1981).
[19] P. Peczak, A. L. Ferrenberg, and D. P. Landau, Phys. Rev. B **43**, 6087 (1991).
[20] W. H. Press, B. P. Flannery, S. A. Teukolsky, and W. T. Vetterling, in *Numerical Recipes—The Art of Scientific Computing* (Cambridge University Press, Cambridge, England, 1986).